Since January 2020 Elsevier has created a COVID-19 resource centre with free information in English and Mandarin on the novel coronavirus COVID-19. The COVID-19 resource centre is hosted on Elsevier Connect, the company's public news and information website.

Elsevier hereby grants permission to make all its COVID-19-related research that is available on the COVID-19 resource centre - including this research content - immediately available in PubMed Central and other publicly funded repositories, such as the WHO COVID database with rights for unrestricted research re-use and analyses in any form or by any means with acknowledgement of the original source. These permissions are granted for free by Elsevier for as long as the COVID-19 resource centre remains active.

Chemosphere 270 (2021) 129435

Contents lists available at ScienceDirect

Chemosphere

journal homepage: www.elsevier.com/locate/chemosphere

Variations in Black Carbon concentration and sources during COVID-19 lockdown in Delhi

Vikas Goel [a], Naba Hazarika [b], Mayank Kumar [a, *], Vikram Singh [c, **], Navaneeth M. Thamban [d], Sachchida Nand Tripathi [d, ***]

[a] Department of Mechanical Engineering, Indian Institute of Technology Delhi, New Delhi, 110016, India
[b] Department of Applied Mechanics, Indian Institute of Technology Delhi, New Delhi, 110016, India
[c] Department of Chemical Engineering, Indian Institute of Technology Delhi, New Delhi, 110016, India
[d] Department of Civil Engineering, Indian Institute of Technology Kanpur, Uttar Pradesh, 208016, India

HIGHLIGHTS

- Concentration of BC varied from 0.22 to 16.92 μg/m^3 throughout the entire study period.
- BC concentration decreased up to 78% during lockdown as compared to pre-lockdown phase.
- Fossil fuel (BC_{ff}) emissions dominated over those from biomass burning (BC_{bb}).
- Trajectory and CWT analyses indicated maximum contribution from local sources.

GRAPHICAL ABSTRACT

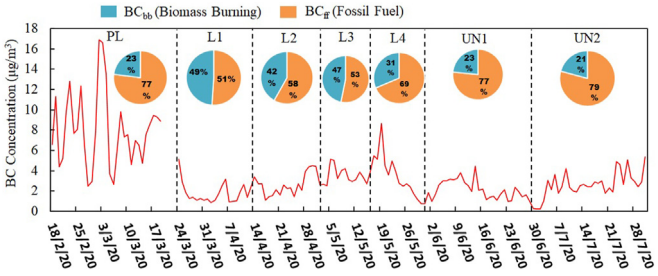

ARTICLE INFO

Article history:
Received 1 October 2020
Received in revised form
18 December 2020
Accepted 22 December 2020
Available online 26 December 2020

Handling Editor: R Ebinghaus

Keywords:
COVID-19
Lockdown
Black carbon
Aethalometer
Source apportionment
Absorption angstrom exponent

ABSTRACT

A nationwide lockdown was imposed in India due to COVID-19 pandemic in five phases from 25th March to May 31, 2020. The lockdown restricted major anthropogenic activities, primarily vehicular and industrial, thereby reducing the particulate matter concentration. This work investigates the variation in Black Carbon (BC) concentration and its sources (primarily Fossil Fuel (ff) burning and Biomass Burning (bb)) over Delhi from 18th February to July 31, 2020, covering one month of pre-lockdown phase, all the lockdown phases, and two months of successive lockdown relaxations. The daily average BC concentration varied from 0.22 to 16.92 μg/m^3, with a mean value of 3.62 ± 2.93 μg/m^3. During Pre-Lockdown (PL, 18th Feb-24th March 2020), Lockdown-1 (L1, 25th March-14th April 2020), Lockdown-2 (L2, 15th April-3rd May 2020), Lockdown-3 (L3, 4th-17th May 2020), Lockdown-4 (L4, 18th-31st May 2020), Unlock-1 (UN1, June 2020), and Unlock-2 (UN2, July 2020) the average BC concentrations were 7.93, 1.73, 2.59, 3.76, 3.26, 2.07, and 2.70 μg/m^3, respectively. During the lockdown and unlock phases, BC decreased up to 78% compared to the PL period. The BC source apportionment studies show that fossil fuel burning was the dominant BC source during the entire sampling period. From L1 to UN2 an increasing trend in BC_{ff} contribution was observed (except L3) due to the successive relaxations given to anthropogenic activities. BC_{ff} contribution dipped briefly during L3 due to the intensive crop residue burning events in

* Corresponding author.
** Corresponding author.
*** Corresponding author.
E-mail addresses: kmayank@mech.iitd.ac.in (M. Kumar), vs225@chemical.iitd.ac.in (V. Singh), snt@iitk.ac.in (S.N. Tripathi).

https://doi.org/10.1016/j.chemosphere.2020.129435
0045-6535/© 2020 Elsevier Ltd. All rights reserved.

neighboring states. CWT analysis showed that local emission sources were the dominant contributors to BC concentration over Delhi.

© 2020 Elsevier Ltd. All rights reserved.

1. Introduction

Black Carbon (BC) strongly absorbs solar radiation and causes positive radiative forcing due to the high value of the imaginary part of its refractive index (Bond et al., 2013; Goel et al., 2020). It affects the Earth's radiation budget through direct, semidirect, and indirect effects. Major sources of BC in the atmosphere are incomplete combustion of fossil fuel, biomass, etc. (Bikkina et al., 2019; Dumka et al., 2018). BC/Particulate Matter (PM) also has detrimental effects on visibility, air quality, agricultural productivity, ecosystem, human health, and exacerbates global warming (Goel et al., 2018a; Gong et al., 2016; Hazarika et al., 2017, 2019; Reddington et al., 2013). The deposition of BC particles over glaciers contributes to their premature thawing and fragmentation as it produces the albedo effect that accelerates snow melting (Menon et al., 2010; Zhang et al., 2020). Recently, BC has achieved much attention because of its high global warming potential, second only to carbon dioxide (CO_2), with a total climate forcing of +1.1 W m^{-2} (0.17–2.1 W m^{-2}) and short lifetime (<5 days) in the atmosphere (Bond et al., 2013; Stocker, 2014).

The current COVID-19 pandemic has forced the governments of different nations to impose countrywide partial or complete lockdown, limiting anthropogenic activities to a larger extent. The deadly Severe Acute Respiratory Syndrome Coronavirus 2 (SARS-CoV-2) has globally caused more than 0.8 million deaths, and more than 24 million confirmed patients (https://www.who.int/emergencies/diseases/novel-coronavirus-2019). In India, to contain the spread of SARS-CoV-2, a nationwide lockdown was implemented from 25th March till May 31, 2020, in different phases. Due to lockdown, a significant decrease in vehicular movement, construction work, industrial and other commercial activities was noticed across the country, which reduced the $PM_{2.5}$ (particulate matter with an aerodynamic diameter less than 2.5 μm) and PM_{10} (particulate matter with an aerodynamic diameter less than 10 μm) concentration in Indian megacities, e.g., Delhi (Dhaka et al., 2020; Mahato et al., 2020; Singh and Chauhan, 2020). According to a study conducted by Mahato et al. (2020), $PM_{2.5}$ and PM_{10} mass concentrations reduced by 39% and 60%, respectively, during the first phase of lockdown (25th March – April 14, 2020) in Delhi as compared to last year (2019), due to the imposed restrictions on diverse anthropogenic activities. To the best of our knowledge, this is the first study over Delhi where the effect of lockdown on BC concentration and its source contribution is discussed during the pandemic.

Delhi is a typical urban city where fossil fuel (ff) combustion and biomass burning (bb) are the two primary sources of BC (Dumka et al., 2018; Bikkina et al., 2019; Kumar et al., 2020). Previous studies have shown that the contribution of BC_{ff} and BC_{bb} to the BC in Delhi varies from 72 to 94% and 6–28%, respectively (Bikkina et al., 2019; Dumka et al., 2018; Tiwari et al., 2015). The current study reports the variation in BC concentration, sources, and their contributions due to the lockdown in Delhi. The BC measurements were carried out using a seven-channel aethalometer, and the BC source apportionment was carried out using the Aethalometer model discussed by Sandradewi et al. (2008). The BC concentration at 880 nm was used as a representative of total BC, and the source apportionment was carried out using the 370 and 880 wavelength pair. The main objective of the present study is to investigate the effect of lockdown on temporal (daily and diurnal) variation of BC and its sources. This study provides a detailed information of the BC sources which will help to formulate the BC abatement strategies. Sources apportionment studies have become increasingly important, which can provide details and cognizance about the influential emission sources present in and around the receptor location (Hopke et al., 2020). The source apportionment of BC has a prime importance to understand its chemistry and in developing the air pollution mitigation strategies because it has potential to offset the CO_2 induced warming in near future due to its shorter lifetime.

2. Experimental section

2.1. Sampling site

The BC measurement was done at an urban site in Delhi (Indian Institute of Technology Delhi, IITD) (28°32′N; 77°11′E) from 18th February – March 19, 2020, and 24th March – July 31, 2020. During the measurements, sampling interruption occurred between 20th –22nd March 2020. The continuous real-time BC measurement was performed with the help of a seven-channel Magee® AE33 aethalometer installed at the height of nearly 15 m from the ground. The instrument was operated at a flow rate of 2 LPM with $PM_{2.5}$ inlet and was subjected to measure BC mass concentration in 1 min interval. The sampling site is not directly influenced by any larger industrial hub but experiences intensive vehicular activities due to the nearby national highway. Further details of the sampling site can be found elsewhere (Rai et al., 2020).

To prevent the spread of SARS-CoV-2 a nationwide lockdown was imposed all over India. The lockdown was implemented in different phases, along with implementing restrictions in various activities from 25th March – May 31, 2020. After 31st May, the lockdown was lifted under the name Unlock-1 which was first implemented from 1st - 30th June then extended till July 31, 2020 (Unlock-2). Initially, the lockdown was implemented from 25th March to April 14, 2020, which was later extended to subsequent phases till May 31, 2020. Each set of lockdown periods has a unique set of relaxations in various activities. Therefore, the sampling period was also divided into different phases; Pre-Lockdown (PL, 18th Feb-24th March 2020), Lockdown Phase 1 (L1, 25th March-14th April 2020), Lockdown Phase 2 (L2, 15th April – May 3, 2020), Lockdown Phase 3 (L3, 4th –17th May 2020), Lockdown Phase 4 (L4, 18th –31st May 2020), Unlock 1 (UN1, 1st –30th June 2020), and Unlock-2 (UN2, 1st –31st July 2020).

2.2. Methods

2.2.1. BC measurement

AE33 measures light attenuation at 370, 470, 520, 590, 660, 880, and 950 nm, which is linearly proportional to the BC deposited over the filter tape (Hansen et al., 1984). The instrument uses the dual spot technology. The incoming stream of air is divided into two streams with unequal flow rates and passes through two spots on the same filter tape, thus providing light attenuation simultaneously (Drinovec et al., 2015). Uncertainties in the BC measurements of aethalometer may arise from multiple scattering of light

in the filter tape when the filter is relatively unloaded, and due to the shadowing effect which occurs when the filter gets heavily loaded (Collaud Coen et al., 2010; Weingartner et al., 2003). According to Weingartner et al. (2003), the shadowing effect is predominant in pure BC, not in the case of mixed BC (i.e., the mixture of different aerosols). The sampling site in the present study is a typical urban that predominantly has a mixed BC (Ahlawat et al., 2019; Mishra et al., 2018), so the corrections regarding the shadowing effect are not required in the present case. More details of the aethalometer can be obtained elsewhere (Hansen et al., 1984; Ramachandran and Rajesh, 2007). The 24-hourly average BC concentration was calculated at 880 nm, as it is considered as a true representative of the BC concentration in the atmosphere. At 880 nm, BC is the principal absorber of light, and other species have negligible absorption (Bodhaine, 1995; Goel et al., 2018b). Biomass burning and vehicular emissions are regarded as the two primary sources of BC (Dumka et al., 2018; Saraswat et al., 2013; Tiwari et al., 2013). The instrument used in the present study is well maintained and calibrated, the flow test, leakage test, sampling spot test, optical chamber cleaning and inlet cleaning were performed periodically as per the user manual of the instrument. These parameters directly influence accuracy of the instrument (Cuesta et al., 2020).

2.2.2. Absorption angstrom exponent

Absorption Angstrom Exponent (AAE) is a wavelength-dependent aerosol optical property, calculated from the aerosol absorption coefficient (b_{abs}), which is a product of BC concentration and Mass Absorption Efficiency (MAE). MAE for 370, 470, 880, and 950 nm wavelengths are 18.47, 14.54, 7.77, and 7.19 m^2g^{-1}, respectively (as provided by the instrument manufacturer). In the present study, AAE values were calculated for two-wavelength pairs (370 and 880 nm, and 470 and 950 nm) using the following equations,

$$b_{abs} = BC \times MAE \tag{1}$$

$$AAE = -\frac{ln(b_{abs1}/\, b_{abs2})}{\ln(\lambda_1/\lambda_2)} \tag{2}$$

Here, b_{abs1} and b_{abs2} are the absorption coefficients at wavelengths, λ_1, and λ_2.

2.2.3. Aethalometer model

The aethalometer model is widely used for the source apportionment of BC (Dumka et al., 2018; Helin et al., 2018; Jing et al., 2019; Ravi Kiran et al., 2019; Sandradewi et al., 2008; Tobler et al., 2020). The functioning of the model depends on the light absorption by BC at near UV and near IR regions. The BC coming from the biomass burning sources consists of organic aerosols that show strong absorption in the UV region than that of near-infrared range. The fossil fuel emissions are generally composed of BC, which shows strong absorption near the 880 nm (near-IR region) wavelength. Therefore, the multi-wavelength (ranging from 370 nm to 950 nm) aethalometer could be used to bifurcate the BC sources into biomass and fossil fuel-based on the spectral dependency of b_{abs}, which is defined as:

$$b_{abs} \sim \lambda^{-\alpha} \tag{3}$$

where λ is the wavelength, and α is AAE. Many studies have calculated the AAE for biomass burning and reported it to vary between 0.9 and 2.2, which strongly depends upon the type of the wood used for burning and the burning conditions (Day et al., 2006; Martinsson et al., 2017; Mousavi et al., 2019; Sandradewi et al., 2008). While, for AAE fossil fuel, there is a fair consensus among the scientific community that it does not significantly vary and lies between 0.8 and 1.1 (Schnaiter et al., 2003; Kirchstetter et al., 2004; Schnaiter, 2005; Drinovec et al., 2015). The BC source apportionment calculations were done considering AAE of ff as 1 and bb as 1.8. Similar values were used by Dumka et al. (2018) for BC source apportionment over Delhi. Earlier studies have reported the 370 nm and 880 nm wavelength pair to be the most accurate for the BC source apportionment (Dumka et al., 2018; Garg et al., 2016; Mousavi et al., 2019; Vaishya et al., 2017), and the same has been used in the present study. The BC source apportionment was carried out with the help of equations (4)–(9), using the absorption coefficients calculated for 370 nm and 880 nm wavelengths. The absorption coefficients were calculated using the BC mass concentrations at 370 and 880 nm wavelengths with the help of eq (1). Equation (4) and (5) were derived on the basis of Beer-Lambert's law, relating the absorption coefficient (b_{abs}), wavelength (λ) and absorption angstrom exponent (α) for the pure fossil fuel and biomass burning activities (Sandradewi et al., 2008).

$$\frac{b_{abs,ff,370}}{b_{abs,bb,880}} = \left(\frac{370}{880}\right)^{\propto_{ff}} \tag{4}$$

$$\frac{b_{abs,bb,370}}{b_{abs,bb,880}} = \left(\frac{370}{880}\right)^{-\propto_{bb}} \tag{5}$$

$$b_{abs,\lambda} = b_{abs,ff,\lambda} + b_{abs,bb,\lambda} \tag{6}$$

$$BC_{ff} = \frac{b_{abs,ff,880}}{MAC_{880}} \tag{7}$$

$$BC_{bb} = \frac{b_{abs,bb,880}}{MAC_{880}} \tag{8}$$

$$BC = BC_{ff} + BC_{bb} \tag{9}$$

where, $b_{abs,\lambda}$ is an aerosol absorption coefficient at λ. $b_{abs,ff,\lambda}$ and $b_{abs,bb,\lambda}$ are the aerosol absorption coefficients of fossil fuel and biomass at λ; $b_{abs,ff,370}$ and $b_{abs,ff,880}$ are aerosol absorption coefficient of fossil fuel BC at 370 and 880 nm, respectively. Similarly, $b_{abs,bb,370}$ and $b_{abs,bb,880}$ are aerosol absorption coefficient of biomass burning BC at 370 and 880 nm, respectively. MAC_{880} is a mass absorption coefficient at 880 nm. BC_{ff} and BC_{bb} are the Black Carbon (BC) concentrations coming from fossil fuel and biomass burning, respectively. The exponents α_{ff} and α_{bb} represent AAE of fossil fuel and biomass burning, respectively.

2.3. Backward wind trajectory and CWT analysis

To find out the transboundary movement of BC at the receptor site from potential sources, 72 h backward wind trajectories were plotted at the height of 100 m AMSL for the entire sampling period. The trajectories were plotted with the help of the Hybrid Single-Particle Lagrangian Integrated Trajectory (HYSPLIT) model developed by the National Oceanic and Atmospheric Administration (NOAA) Air Resource Laboratory's (ARL) (http://ready.arl.noaa.gov/HYSPLIT.php) with the Global Data Assimilation System (GDAS) data as input.

The potential source regions contributing to the BC concentration at the receptor site were identified with the help of the Concentration Weighted Trajectories (CWT) analysis (Goel et al., 2020; Jain et al., 2017). Potential source regions surrounding the receptor site were divided into *ij*th gridded array. CWT is a function of BC concentration and time spent by the trajectory in *ij*th grid, which is defined as Eq (10):

$$C_{ij} = \frac{1}{\sum_{l=1}^{M} \tau_{ijl}} \sum_{l=1}^{M} C_l \tau_{ijl} \quad (10)$$

Here, C_{ij} is the mean weighted concentration at the ijth grid, M is a total number of trajectories, C_l is a measured concentration at the receptor site on the arrival of the trajectory l, and τ_{ijl} is the time spend in the ijth grid cell associated with the C_l sample.

3. Result and discussion

3.1. BC concentration

3.1.1. Temporal and diurnal variation of BC concentrations

The temporal and diurnal variations of BC concentration are shown in Fig. 1 (a and b). In the entire sampling period, the BC concentration varied from 0.22 to 16.92 μg/m^3, with a mean concentration of 3.62 ± 2.93 μg/m^3. The maximum concentration was observed in the PL period (on March 2, 2020), and the minimum concentration was observed in UN2 (on July 1, 2020). The average BC concentrations during PL, L1, L2, L3, L4, UN1, and UN2 were 7.93, 1.73, 2.59, 3.76, 3.26, 2.07, and 2.70 μg/m^3, respectively. The BC concentration observed during PL was comparable to BC reported in the earlier studies ~8 μg/m^3 (Bikkina et al., 2019; Tobler et al., 2020). The BC concentration during March, April, and May 2020 was ~35%, ~77%, and ~52% lower than the BC reported during similar months in 2018 (Tobler et al., 2020). The BC concentration observed during UN1 (June 2020) and UN2 (July 2020) was ~59% and ~27% lower than the BC measured during a similar period in 2017 (Tyagi et al., 2020). During L1, L2, L3, L4, UN1, and UN2, the BC concentration compared to PL was reduce by 78%, 67%, 53%, 59%, 74%, and 66%, respectively, due to the decrease BC emissions. Among the specified phases, the maximum concentration was observed during PL, whereas it was minimum during the UN2 period. An increasing trend in the BC concentration from L1 to L3 was due to the phase-wise relaxations given in successive lockdowns. However, after L3, the BC concentration decreased due to the high wind speed, high temperature, and rain events during this period. Delhi experiences heavy rainfall and high wind speed in June and July, which decreases the PM/BC concentrations (Jain et al., 2020; Sharma et al., 2018). During UN1 and UN2, the direction of the wind parcel changes, and the strong monsoonal winds are one of the reasons for decreased BC concentration (Fig, S1, supplementary information).

The diurnal variation of BC concentration is shown in the contour plot (Fig. 1b). The morning and evening peaks of the BC concentration are visible in the PL period, primarily driven by high vehicular emissions and low boundary layer height during the morning and evening hours. The BC concentration during the PL period between 10:00 h and 18:00 h decreased up to ~4 μg/m^3 due to the increased boundary layer height and low vehicular emissions. In the afternoon hours, the strong convective air pushed the boundary layer upward, which decreases the ambient aerosol concentration. In the L1 and L2 periods, the intensity of both morning and evening peaks decreased to ~2 μg/m^3 due to the minimal vehicular emissions. In the L3 and L4 periods, the morning and evening peaks again started reappearing, with less intensity than the Pre-Lockdown period due to the biomass burning activities that occurred in the Punjab and Haryana regions in northern India during this period. During UN1 and UN2, the intensity of the peaks again decreased due to high wind speed and rain events that occurred during this period.

3.2. Diurnal variation of AAE

AAE is an important optical property of light-absorbing aerosol particles used for aerosol characterization and source apportionment. AAE gives information about the particle's shape, size, and chemical composition. AAE near to 1 implies the BC particles coming from fossil fuel combustion sources, whereas higher AAE corresponds to organic aerosols from the biomass burning sources (Russell et al., 2010). AAE is widely used to quantitatively distinguish the brown carbon absorption from BC absorption (Kirchstetter and Thatcher, 2012; Liu et al., 2015). Diurnal variations of AAE calculated for two-wavelength pairs (370–880 nm, 470–950 nm) are shown in Fig. 2 (a and b). The significant daily and diurnal variations in calculated AAE indicated the variation in composition and relative source contribution of light-absorbing aerosols to the BC. During the entire sampling period, $AAE_{370\text{-}880}$ varied from 1.13 to 2.42 with a mean value of 1.32 ± 0.16 (Fig. 2a), which is lower than the AAE value (1.9 ± 0.1) reported over Delhi during wintertime by Ganguly et al. (2006), and higher than the Tiwari et al. (2015), i.e., 1.09 ± 0.11 measured during December 2011–March 2012. The AAE values reported in the present study

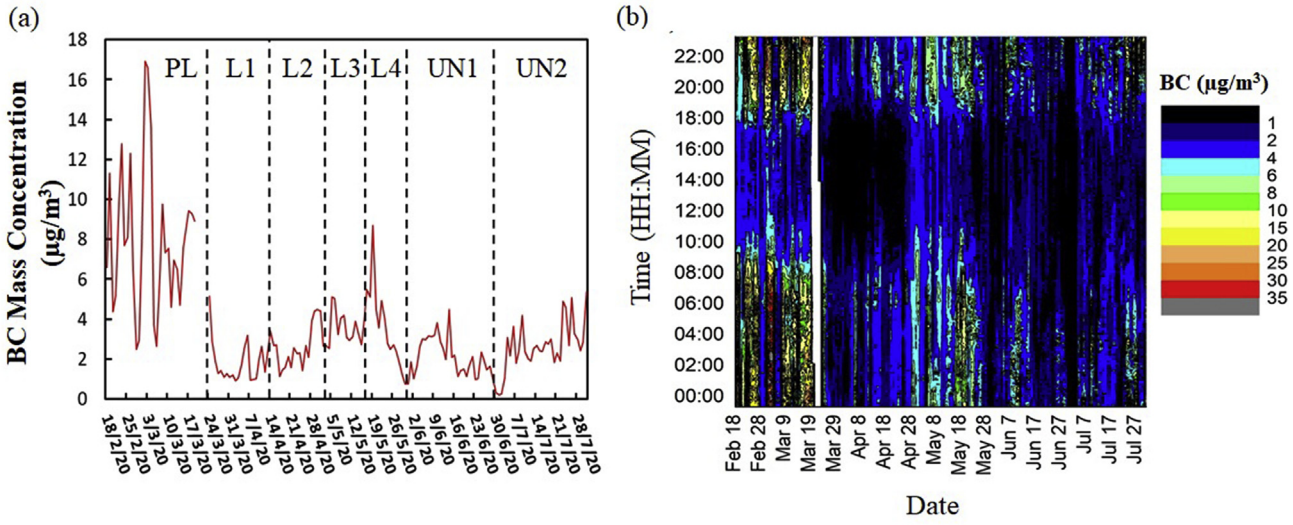

Fig. 1. (a) Temporal variation of BC mass concentration and (b) the daily-diurnal variation of BC using contour plot.

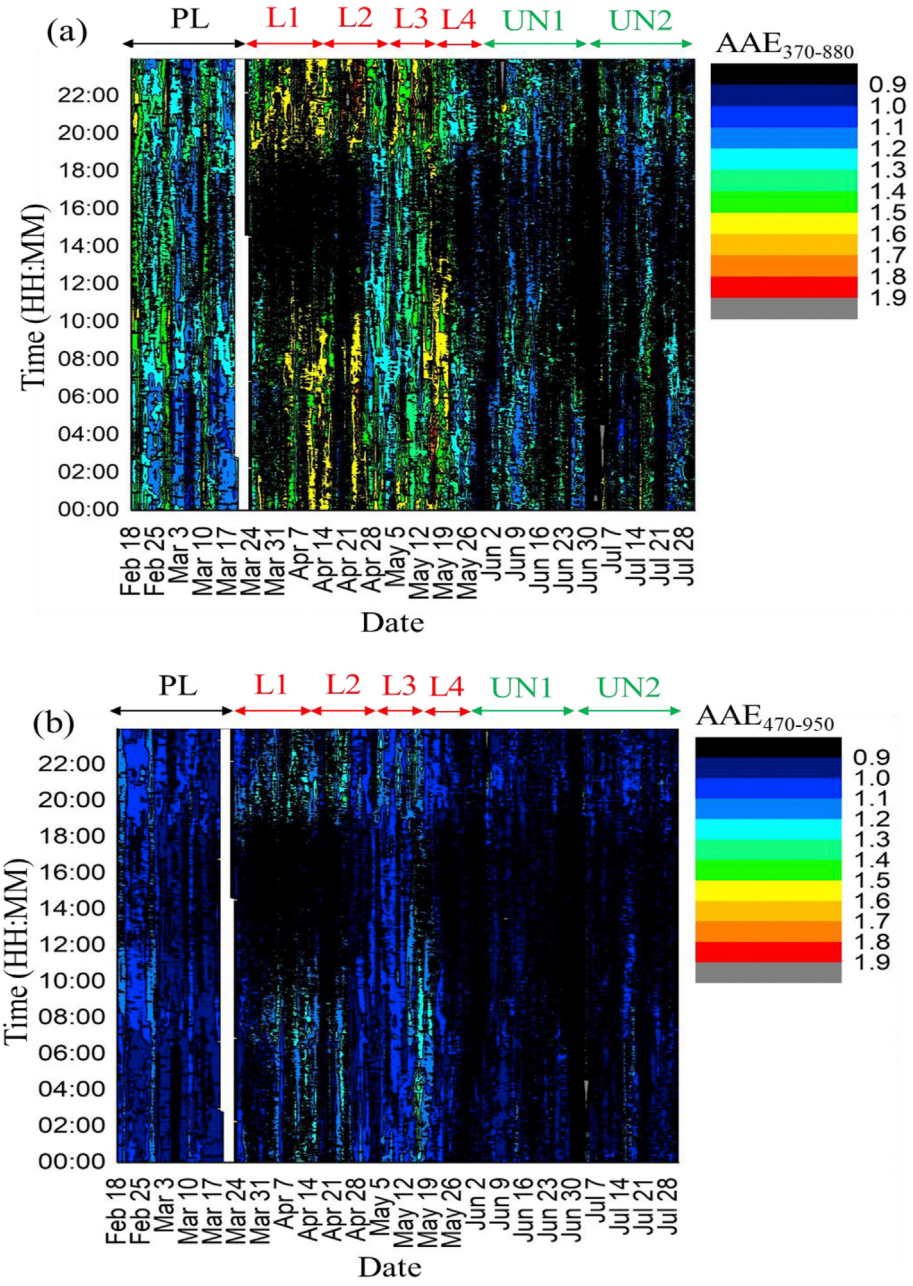

Fig. 2. Diurnal contour plots of (a) $AAE_{370\text{-}880}$ and (b) $AAE_{470\text{-}950}$.

are comparable to the AAE values (1.29 ± 0.08) reported by Dumka et al. (2018) over Delhi from December 2015–February 2016. The average $AAE_{370\text{-}880}$ during PL, L1, L2, L3, L4, UN1, and UN2 were 1.25, 1.46, 1.41, 1.44, 1.26, 1.24, and 1.27, respectively. The higher value of $AAE_{370\text{-}880}$ during L1, L2, and L3 shows the elevated contribution from biomass burning sources and the low $AAE_{370\text{-}880}$ values during PL, L4, UN1 and UN2 are suggesting the major contribution from fossil fuel combustion sources. The $AAE_{470\text{-}950}$ was observed to vary from 0.81 to 2.16 with a mean value of 1.04 ± 0.12 (Fig. 2b). The average $AAE_{470\text{-}950}$ during PL, L1, L2, L3, L4, UN1, and UN2 was observed 1.01, 1.13, 1.09, 1.10, 1.01, 1.00, and 1.03, respectively.

3.3. BC source apportionment

Source apportionment of BC was done using the Aethalometer model discussed in section 2.3. The source apportionment was done using 370 nm and 880 nm wavelength pair and considering α_{ff} and α_{bb} as 1 and 1.8, respectively (Dumka et al., 2018). The source apportionment results are shown in Fig. 3. The average BC_{ff} concentrations during PL, L1, L2, L3, L4, UN1, and UN2 were 5.9, 0.88, 1.48, 2.00, 2.18, 1.59, and 2.12 μg/m^3, respectively. The BC_{ff} concentration was highest during PL than other phases as there were no restrictions on vehicular, industrial, or any other anthropogenic activities (Fig. 3a). Whereas, during the lockdown, strict laws were enforced, which restricted the movement of public vehicles except the vehicles used for essential services (doctors, essential commodities, police, etc.). During L1, the BC_{ff} was significantly decreased to 0.88 μg/m^3 because of the complete restriction on anthropogenic activities. However, an increasing trend in BC_{ff} concentration was observed from L1 to L4, due to the successive

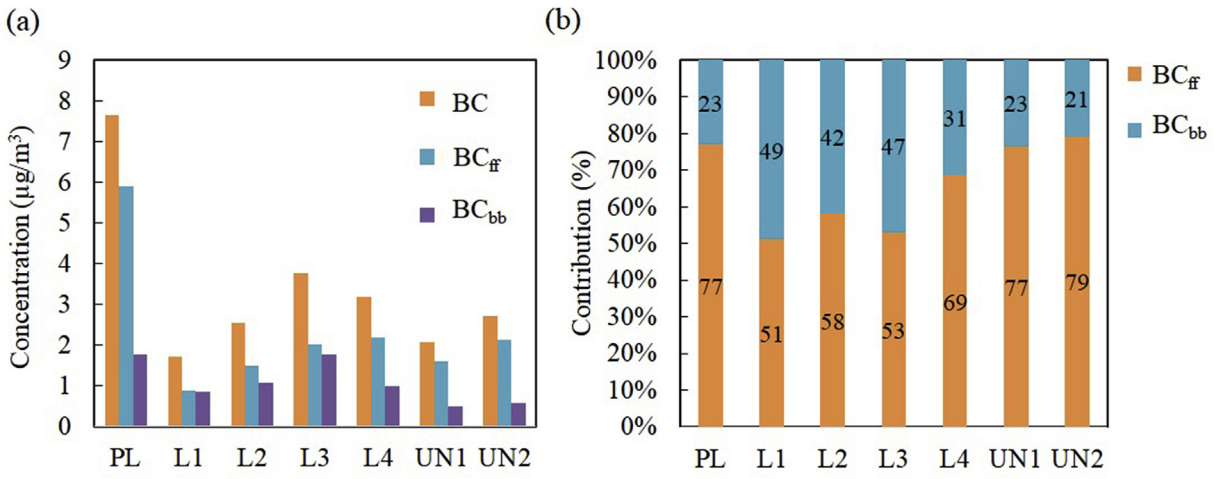

Fig. 3. (a) Mass concentration of BC, BC_{ff} and BC_{bb} observed during PL, L1, L2, L3, L4, UN1, and UN2, (b) contribution of BC_{ff} and BC_{bb} in BC during different phases.

relaxations of diverse man-made activities in lockdown. Google mobility report data of transit stations has also shown a similar trend, reinforcing the findings of the present study (Fig. 4a). Despite the more relaxations in UN1 and UN2, BC_{ff} concentration during UN1 and UN2 has reduced compared to L4 due to the increased wind speed and rain events during this period (Jain et al., 2020; Sharma et al., 2018). The average BC_{bb} concentrations during the PL, L1, L2, L3, L4, UN1 and UN2 were 1.76, 0.84, 1.06, 1.76, 0.99, 0.49, and 0.56 μg/m^3, respectively. BC_{bb} was high during L3 and L4 due to the crop residue burning events that occurred in the northern region of India during that time. During L3 and L4, the potential source regions of BC lie in the Punjab, Haryana, parts of Pakistan, and Indo-Gangetic Plains (IGP), where intensive crop residue burning activities were observed (Fig. 5 d and e).

The contributions of BC_{ff} and BC_{bb} to the total BC during PL, L1, L2, L3, L4, UN1, and UN2 are shown in Fig. 3b. The BC_{ff} contribution to the total BC was high during PL, UN1, and UN2, i.e., 77%, 77%, and 79%, respectively. The high BC_{ff} contribution during PL is due to the non-restriction on anthropogenic activities, e.g., vehicular, industrial, etc. During UN1 and UN2, the BC_{ff} contribution was comparable with PL due to the relaxations given during that period. During UN1 and UN2, the Delhi Metro, a major mode of commute for Delhi people was not operational, which consequently led to an increment of private vehicles. From L1 to UN2, an increasing trend in BC_{ff} contribution was observed (except L3), which is due to the relaxations given in successive lockdowns and unlocks. During L3, BC_{ff} contribution decreased due to the crop residue burning events in Punjab, Haryana, and parts of Uttar Pradesh during this period. Moderate Resolution Imaging Spectroradiometer (MODIS) satellite-derived Fire Information for Resource Management System (FIRMS) data plotted with the BC_{bb} mass concentration confirms the higher numbers of fire events during that period (Fig. 4b). However, a

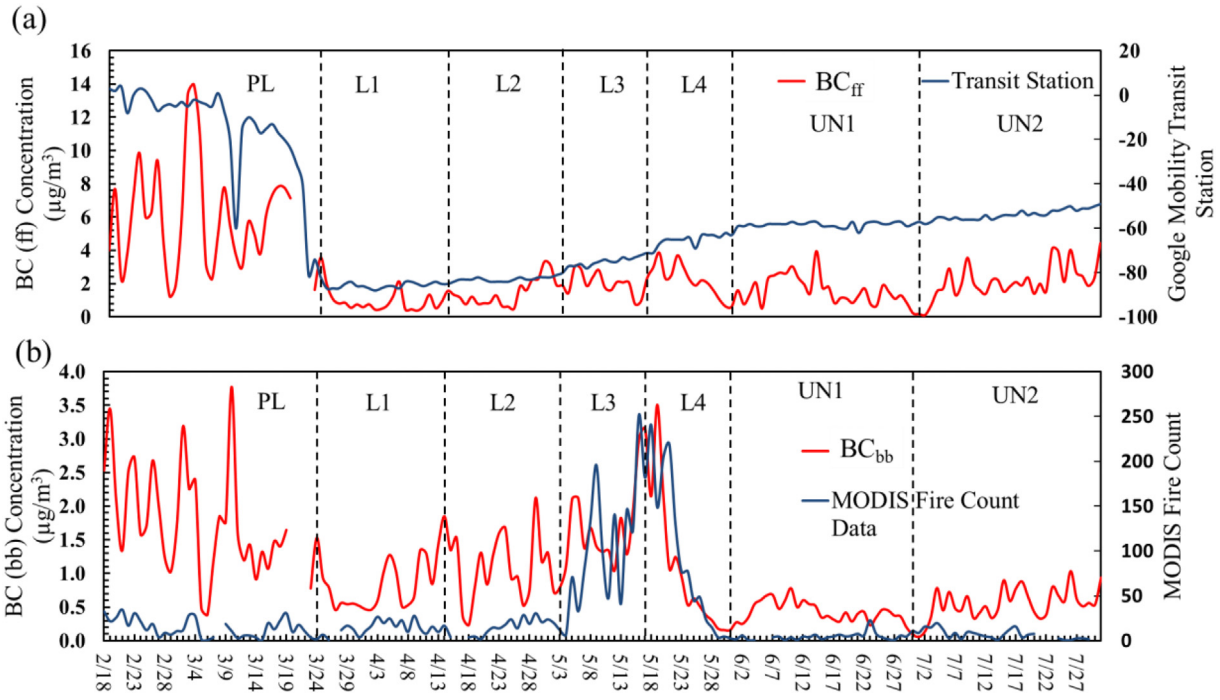

Fig. 4. Temporal variation of (a) BC_{ff} and Google mobility transit station data, and (b) BC_{bb} and MODIS fire counts.

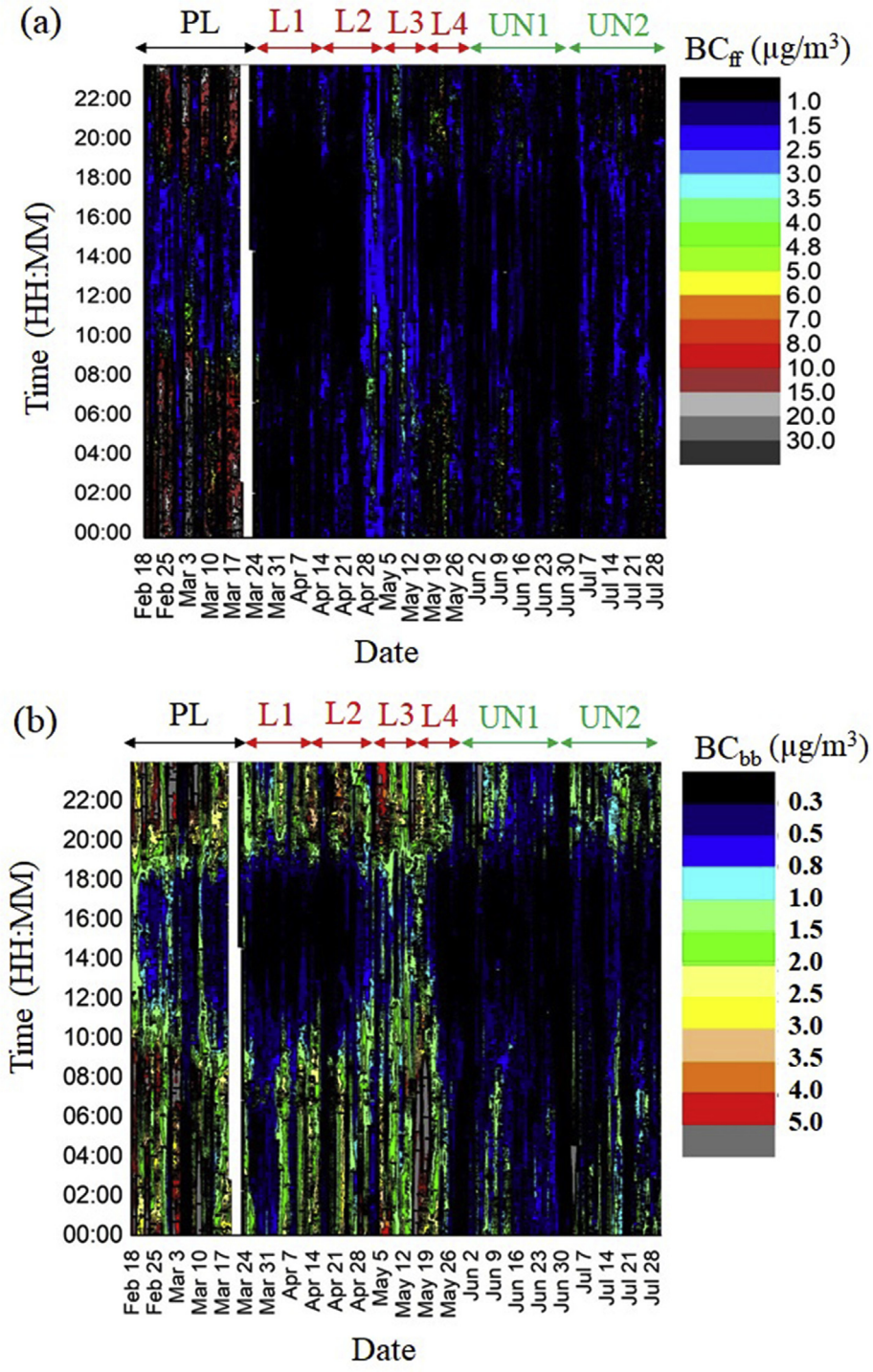

Fig. 5. Diurnal variation of (a) BC_{ff}, and (b) BC_{bb}.

contrasting trend was observed in BC_{bb} contribution, which was highest during L1 and lowest during UN2. BC_{bb} contribution was high during L1 and L3 due to decreased vehicular emission during L1 and increased crop residue burning activities during L3.

3.4. Temporal and diurnal variation of BC_{ff} and BC_{bb}

During the entire sampling period, the daily average BC_{ff} mass concentration varied from 0.1 to 14.0 μg/m^3, with a mean value of 2.6 ± 2.36 μg/m^3 (Fig. 4a). The BC_{ff} mass concentration was high during PL, which decrease substantially in different lockdown phases. The daily average BC_{bb} concentration varied from 0.05 to 3.77 μg/m^3, with a mean value of 1.02 ± 0.76 μg/m^3 (Fig. 4b). Intense BC_{bb} concentration peaks during L3 and L4 were observed probably due to the crop residue burning events in India's northern region (particularly in Punjab and Haryana) during that period. Whereas, the decrease in BC_{bb} concentration during UN1 and UN2 period could be attributed to the prevailing meteorology like high rainfall,

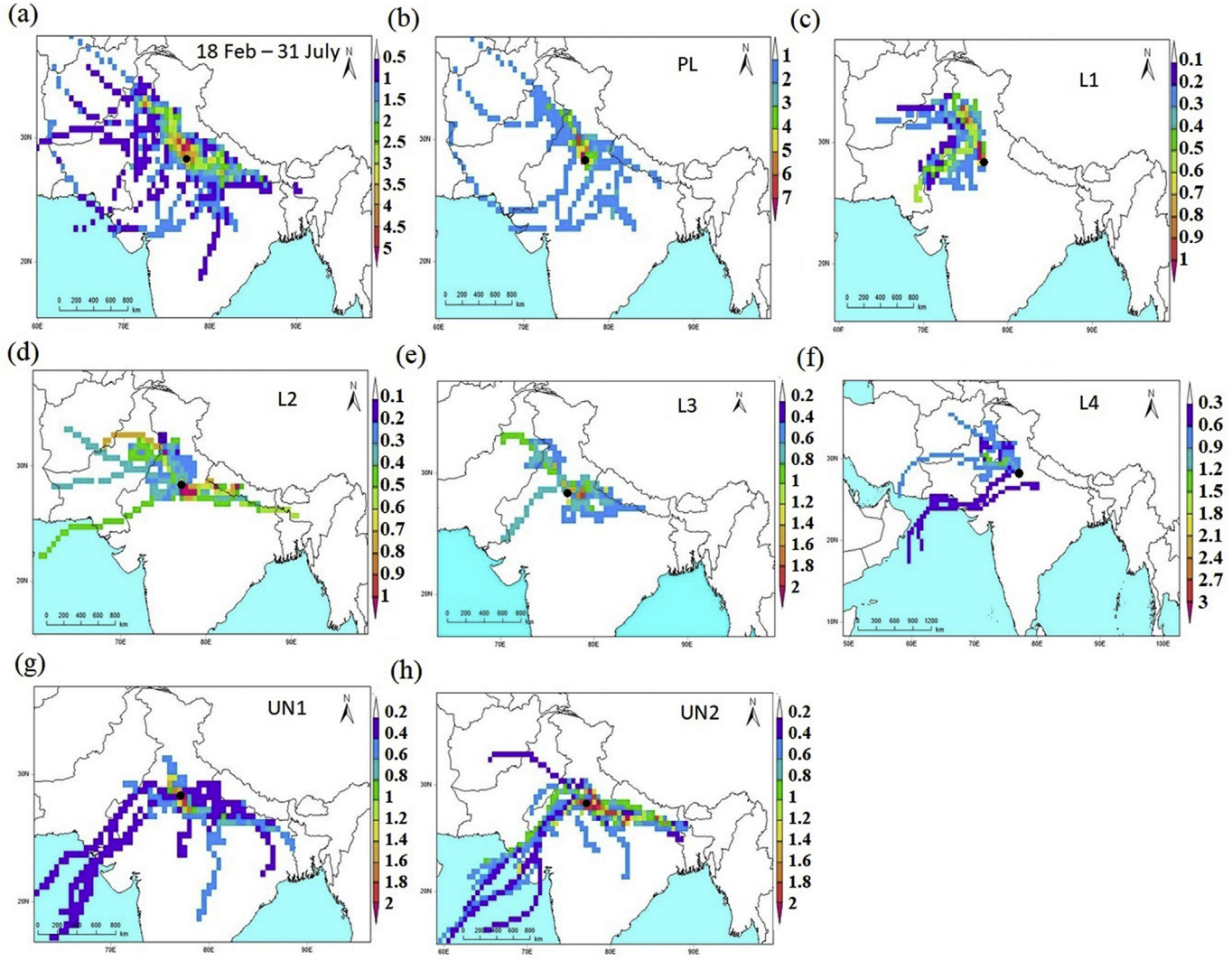

Fig. 6. Maps of concentration weighted trajectories for the complete sampling period (a)18 Feb-31 July 2020, (b) PL, (c) L1, (d) L2, (e) L3, (f) L4, (g) UN1, and (h) UN2 phases. The values shown in the legend represents the BC mass concentration in μg/m^3.

high wind speed, and change in wind direction (Figure S1; supplementary information).

Diurnal contour plots of BC_{bb} and BC_{ff} are shown in Fig. 5(a and b). Intense BC_{ff} concentration peaks were observed during morning and evening hours of PL period, a characteristic of high vehicular emission and low boundary layer height during these hours. High BC_{ff} concentration (10–20 μg/m^3) was observed during morning and evening hours, which gradually decreased to ~1.5–2.5 μg/m^3 in the afternoon hours (12:00–18:00) during the PL period (Fig. 5a). The morning and evening peaks of BC_{ff} were rarely observed during L1, L2, L3, L4, UN1, and UN2 due to the traffic movement restrictions. However, a contrasting pattern was observed in the contour plot of BC_{bb} (Fig. 5b), where the morning and evening peaks were visible till L4. This could be attributed to the non-restrictions on biomass burning activities during the lockdown and elevated crop residue burning events in the Punjab and Haryana regions during L3 and L4. The intensity of the BC_{bb} peaks was decreased during UN1 and UN2 due to the variation in meteorological parameters (increased wind speed and rain events) (Sharma et al., 2018).

3.5. Concentration weighted trajectories analysis

Maps of CWT analysis for an entire sampling period, i.e., 18th Feb-31st July 2020 (except 20th –23rd July 2020), PL, L1, L2, L3, L4, UN1, and UN2 periods are shown in Fig. 6. The maps of backward wind trajectories for the same periods are shown in the supplementary information (Fig. S1, supplementary information). During the entire sampling period, stronger to moderate BC source regions were located in the northwest direction (Punjab and Haryana). As discussed earlier, during mid-April-May, the events of crop residue burning are generally high in the parts of Punjab and Haryana, which is one of the primary reasons behind the elevated concentration of BC over the Delhi. The same is being evident from the CWT analysis (Fig. 6a). While moderate to low-value grid cells were spread across the parts of Uttar Pradesh. The potential source regions of BC at the receptor site during the PL period were the parts of Uttar Pradesh, the North-western region (Punjab and Haryana) of India and Pakistan (Fig. 6b). During L1, the major sources of BC were present in/around Rajasthan, Haryana, and Punjab (Fig. 6c). During L2, the major emissions of BC were coming from Pakistan, Punjab, Rajasthan, and the parts of Indo-Gangetic Plain (IGP) region

(Fig. 6d). During L3; Pakistan, Punjab, Haryana, and parts of IGP were the potential source regions of BC (Fig. 6e). During L4, the BC was coming from Punjab, Haryana, and parts of Pakistan (Fig. 6f). During UN1, Haryana and other surrounding regions of Delhi were major source regions of BC (Fig. 6g), and during UN2, BC was primarily coming from the entire IGP belt of India (Fig. 6h). It is to be noted that the strongest emissions sources were present in and around the receptor location, which showed that local sources played a significant role in contributing to the loading of BC over-Delhi (Fig. 6 a, b, c, d, g, and h).

4. Conclusion

The COVID-19 lockdown has resulted in the blue sky and reduced BC concentration over Delhi. During the sampling period, the BC mass concentration varied from 0.22 to 16.92 μg/m^3 (mean 3.62 ± 2.93 μg/m^3) and reduced by 78%, 67%, 53%, 59%, 74%, and 66% during L1, L2, L3, L4, UN1 and UN2 in comparison to PL period. Aethalometer model-based source apportionment results showed that BC_{ff} and BC_{bb} mass concentrations varied from 1.2 to 14.0 μg/m^3 (mean 6.1 ± 2.36 μg/m^3) and 0.38–3.77 μg/m^3 (mean 1.80 ± 0.76 μg/m^3), respectively. The fossil fuel BC contribution to BC was maximum during UN2 and minimum during L1. An increasing trend in BC_{ff} contribution to BC was observed due to increased lockdown relaxations in successive lockdowns and unlocks except L3. High BC_{bb} contribution during L3 was due to the increased agricultural waste burning activities in the nearby North Indian states, primarily Punjab, Haryana, and parts of Uttar Pradesh. The $AAE_{370-880}$ and $AAE_{470-950}$ values varied from 1.13 to 2.42 (mean 1.32 ± 0.16) and 0.81 to 2.16 (mean 1.04 ± 0.12), respectively. The present study showed a significant decrease in BC, BC_{ff}, and BC_{bb} mass concentration over Delhi due to the restrictions on vehicular and industrial activities. This study provides a clear understanding of variation in the contribution of BC from fossil fuel and biomass burning sources due to the reduction in various emission sources of BC in Delhi megacity during COVID-19 pandemic. This detailed observation can be used as a baseline to understand the contributions of potential sources to BC.

Credit author statement

Vikas Goel: Investigation, Data curation, Conceptualization, Formal analysis, Visualization, Methodology, Writing – original draft. Naba Hazarika: Data curation, Investigation, Validation, Writing – review & editing. Mayank Kumar: Conceptualization, Supervision, Resources, Funding acquisition, Project administration, Writing – review & editing. Vikram Singh: Methodology, Supervision, Resources, Funding acquisition, Writing – review & editing. Navaneeth M. Thamban: Software, Validation, Writing – review & editing. Sachchida Nand Tripathi: Supervision, Resources, Project administration.

Declaration of competing interest

The authors declare that they have no known competing financial interests or personal relationships that could have appeared to influence the work reported in this paper.

Acknowledgement

Au-thors ac-knowl-edge the Industrial Research & Development (IRD) unit, In-dian In-sti-tute of Tech-nol-ogy (IIT) Delhi (Grant No. 428 IITD/IRD/MI01810G) Ministery of Human Resource Development (MHRD), Government of India and the Central Pollution Control Board (CPCB), Government of India (Grant No. AQM/Source Apportionment EPC project/2017) for the fund-ing sup-port to carry out this research. NH would like to thank IIT Delhi for awarding the In-sti-tu-tional Post-Doc-toral Fel-low-ship.

Appendix A. Supplementary data

Supplementary data to this article can be found online at https://doi.org/10.1016/j.chemosphere.2020.129435.

References

Ahlawat, A., Mishra, S.K., Goel, V., Sharma, C., Singh, B.P., Wiedensohler, A., 2019. Modelling aerosol optical properties over urban environment (New Delhi) constrained with balloon observation. Atmos. Environ. 205, 115–124. https://doi.org/10.1016/j.atmosenv.2019.02.006.

Bikkina, S., Andersson, A., Kirillova, E.N., Holmstrand, H., Tiwari, S., Srivastava, A.K., Bisht, D.S., Gustafsson, Ö., 2019. Air quality in megacity Delhi affected by countryside biomass burning. Nat Sustain 2, 200–205. https://doi.org/10.1038/s41893-019-0219-0.

Bodhaine, B.A., 1995. Aerosol absorption measurements at barrow, mauna loa and the south pole. J. Geophys. Res. 100, 8967. https://doi.org/10.1029/95JD00513.

Bond, T.C., Doherty, S.J., Fahey, D.W., Forster, P.M., Berntsen, T., DeAngelo, B.J., Flanner, M.G., Ghan, S., Kärcher, B., Koch, D., Kinne, S., Kondo, Y., Quinn, P.K., Sarofim, M.C., Schultz, M.G., Schulz, M., Venkataraman, C., Zhang, H., Zhang, S., Bellouin, N., Guttikunda, S.K., Hopke, P.K., Jacobson, M.Z., Kaiser, J.W., Klimont, Z., Lohmann, U., Schwarz, J.P., Shindell, D., Storelvmo, T., Warren, S.G., Zender, C.S., 2013. Bounding the role of black carbon in the climate system: a scientific assessment: black carbon IN the climate system. J. Geophys. Res. Atmos. 118, 5380–5552. https://doi.org/10.1002/jgrd.50171.

Collaud Coen, M., Weingartner, E., Apituley, A., Ceburnis, D., Fierz-Schmidhauser, R., Flentje, H., Henzing, J.S., Jennings, S.G., Moerman, M., Petzold, A., Schmid, O., Baltensperger, U., 2010. Minimizing light absorption measurement artifacts of the Aethalometer: evaluation of five correction algorithms. Atmos. Meas. Tech. 3, 457–474. https://doi.org/10.5194/amt-3-457-2010.

Cuesta-Mosquera, A., Močnik, G., Drinovec, L., Müller, T., Pfeifer, S., Minguillón, M.C., Björn, B., Buckley, P., Dudoitis, V., Fernández-García, J., Fernández-Amado, M., Ferreira De Brito, J., Flentje, H., Heffernan, E., Kalivitis, N., Kalogridis, A.-C., Keernik, H., Marmureanu, L., Luoma, K., Marinoni, A., Pikridas, M., Schauer, G., Serfozo, N., Servomaa, H., Titos, G., Yus-Díez, J., Zioła, N., Wiedensohler, A., 2020. Intercomparison and characterization of 23 Aethalometers under laboratory and ambient air conditions: procedures and unit-to-unit variabilities (preprint). Aerosols/Laboratory Measurement/Validation and Intercomparisons. https://doi.org/10.5194/amt-2020-344.

Day, D.E., Hand, J.L., Carrico, C.M., Engling, G., Malm, W.C., 2006. Humidification factors from laboratory studies of fresh smoke from biomass fuels. J. Geophys. Res. 111, D22202. https://doi.org/10.1029/2006JD007221.

Dhaka, S.K., Chetna Kumar, V., Panwar, V., Dimri, A.P., Singh, N., Patra, P.K., Matsumi, Y., Takigawa, M., Nakayama, T., Yamaji, K., Kajino, M., Misra, P., Hayashida, S., 2020. PM2.5 diminution and haze events over Delhi during the COVID-19 lockdown period: an interplay between the baseline pollution and meteorology. Sci. Rep. 10, 13442. https://doi.org/10.1038/s41598-020-70179-8.

Drinovec, L., Močnik, G., Zotter, P., Prévôt, A.S.H., Ruckstuhl, C., Coz, E., Rupakheti, M., Sciare, J., Müller, T., Wiedensohler, A., Hansen, A.D.A., 2015. The "dual-spot" Aethalometer: an improved measurement of aerosol black carbon with real-time loading compensation. Atmos. Meas. Tech 8, 1965–1979. https://doi.org/10.5194/amt-8-1965-2015.

Dumka, U.C., Kaskaoutis, D.G., Tiwari, S., Safai, P.D., Attri, S.D., Soni, V.K., Singh, N., Mihalopoulos, N., 2018. Assessment of biomass burning and fossil fuel contribution to black carbon concentrations in Delhi during winter. Atmos. Environ. 194, 93–109. https://doi.org/10.1016/j.atmosenv.2018.09.033.

Ganguly, Dilip, Jayaraman, A, Rajesh, T.A., Gadhavi, H, 2006. Wintertime aerosol properties during foggy and nonfoggy days over urban center Delhi and their implications for shortwave radiative forcing. J. Geophys. Res. 111 https://doi.org/10.1029/2005JD007029.

Garg, S., Chandra, B.P., Sinha, V., Sarda-Esteve, R., Gros, V., Sinha, B., 2016. Limitation of the use of the absorption angstrom exponent for source apportionment of equivalent black carbon: a case study from the north west Indo-Gangetic Plain. Environ. Sci. Technol. 50, 814–824. https://doi.org/10.1021/acs.est.5b03868.

Goel, V., Mishra, S.K., Lodhi, N., Singh, S., Ahlawat, A., Gupta, B., Das, R.M., Kotnala, R.K., 2018a. Physico-chemical characterization of individual Antarctic particles: implications to aerosol optics. Atmos. Environ. 192, 173–181. https://doi.org/10.1016/j.atmosenv.2018.07.046.

Goel, V., Mishra, S.K., Ahlawat, A., Sharma, C., Vijayan, N., Radhakrishnan, S.R., Dimri, A.P., Kotnala, R.K., 2018b. Effect of reduced traffic density on characteristics of particulate matter over Delhi. Curr. Sci. 115, 315. https://doi.org/10.18520/cs/v115/i2/315-319.

Goel, V., Mishra, S.K., Pal, P., Ahlawat, A., Vijayan, N., Jain, S., Sharma, C., 2020. Influence of chemical aging on physico-chemical properties of mineral dust particles: a case study of 2016 dust storms over Delhi. Environ. Pollut. 115338 https://doi.org/10.1016/j.envpol.2020.115338.

Gong, X., Zhang, C., Chen, H., Nizkorodov, S.A., Chen, J., Yang, X., 2016. Size

distribution and mixing state of black carbon particles during a heavy air pollution episode in Shanghai. Atmos. Chem. Phys. 16, 5399–5411. https://doi.org/10.5194/acp-16-5399-2016.
Hansen, A.D.A., Rosen, H., Novakov, T., 1984. The aethalometer — an instrument for the real-time measurement of optical absorption by aerosol particles. Sci. Total Environ. 36, 191–196. https://doi.org/10.1016/0048-9697(84)90265-1.
Hazarika, Naba, Das, Arunangshu, Kamal, Vikas, Anwar, Khalid, Srivastava, Arun, Jain, Vinod K., 2019. Particle phase PAHs in the atmosphere of Delhi-NCR: With spatial distribution, source characterization and risk approximation. Atmos. Environ. 200, 329–342. https://doi.org/10.1016/j.atmosenv.2018.11.064.
Hazarika, Naba, Srivastava, Arun, Das, Arunangshu, 2017. Quantification of particle bound metallic load and PAHs in urban environment of Delhi, India: Source and toxicity assessment. Sustain. Cities Soc. 29, 58–67. https://doi.org/10.1016/j.scs.2016.11.010.
Helin, A., Niemi, J.V., Virkkula, A., Pirjola, L., Teinilä, K., Backman, J., Aurela, M., Saarikoski, S., Rönkkö, T., Asmi, E., Timonen, H., 2018. Characteristics and source apportionment of black carbon in the Helsinki metropolitan area, Finland. Atmos. Environ. 190, 87–98. https://doi.org/10.1016/j.atmosenv.2018.07.022.
Hopke, P.K., Dai, Q., Li, L., Feng, Y., 2020. Global review of recent source apportionments for airborne particulate matter. Sci. Total Environ. 740, 140091. https://doi.org/10.1016/j.scitotenv.2020.140091.
Jain, S., Sharma, S.K., Choudhary, N., Masiwal, R., Saxena, M., Sharma, A., Mandal, T.K., Gupta, A., Gupta, N.C., Sharma, C., 2017. Chemical characteristics and source apportionment of PM2.5 using PCA/APCS, UNMIX, and PMF at an urban site of Delhi, India. Environ. Sci. Pollut. Res. 24, 14637–14656. https://doi.org/10.1007/s11356-017-8925-5.
Jain, S., Sharma, S.K., Vijayan, N., Mandal, T.K., 2020. Seasonal characteristics of aerosols (PM2.5 and PM10) and their source apportionment using PMF: a four year study over Delhi, India. Environ. Pollut. 262, 114337. https://doi.org/10.1016/j.envpol.2020.114337.
Jing, A., Zhu, B., Wang, H., Yu, X., An, J., Kang, H., 2019. Source apportionment of black carbon in different seasons in the northern suburb of Nanjing, China. Atmos. Environ. 201, 190–200. https://doi.org/10.1016/j.atmosenv.2018.12.060.
Kirchstetter, T.W., Novakov, T., Hobbs, P.V., 2004. Evidence that the spectral dependence of light absorption by aerosols is affected by organic carbon: spectral light absorption BY aerosols. J. Geophys. Res. 109 n/a-n/a. https://doi.org/10.1029/2004JD004999.
Kirchstetter, T.W., Thatcher, T.L., 2012. Contribution of organic carbon to wood smoke particulate matter absorption of solar radiation. Atmos. Chem. Phys. 12, 6067–6072. https://doi.org/10.5194/acp-12-6067-2012.
Kumar, R.R., Soni, V.K., Jain, M.K., 2020. Evaluation of spatial and temporal heterogeneity of black carbon aerosol mass concentration over India using three year measurements from IMD BC observation network. Sci. Total Environ. 723, 138060. https://doi.org/10.1016/j.scitotenv.2020.138060.
Liu, C., Yin, Y., Hu, F., Jin, H., Sorensen, C.M., 2015. The effects of monomer size distribution on the radiative properties of black carbon aggregates. Aerosol. Sci. Technol. 49, 928–940. https://doi.org/10.1080/02786826.2015.1085953.
Mahato, S., Pal, S., Ghosh, K.G., 2020. Effect of lockdown amid COVID-19 pandemic on air quality of the megacity Delhi, India. Sci. Total Environ. 730, 139086. https://doi.org/10.1016/j.scitotenv.2020.139086.
Martinsson, J., Abdul Azeem, H., Sporre, M.K., Bergström, R., Ahlberg, E., Öström, E., Kristensson, A., Swietlicki, E., Eriksson Stenström, K., 2017. Carbonaceous aerosol source apportionment using the Aethalometer model – evaluation by radiocarbon and levoglucosan analysis at a rural background site in southern Sweden. Atmos. Chem. Phys. 17, 4265–4281. https://doi.org/10.5194/acp-17-4265-2017.
Menon, S., Koch, D., Beig, G., Sahu, S., Fasullo, J., Orlikowski, D., 2010. Black carbon aerosols and the third polar ice cap. Atmos. Chem. Phys. 10, 4559–4571. https://doi.org/10.5194/acp-10-4559-2010.
Mishra, S.K., Ahlawat, A., Khosla, D., Sharma, C., Prasad, M.V.S.N., Singh, S., Gupta, B., Tulsi Sethi, D., Sinha, P.R., Ojha, D.K., Wiedensohler, A., Kotnala, R.K., 2018. Experimental investigation of variations in morphology, composition and mixing-state of boundary layer aerosol: a balloon based study over urban environment (New Delhi). Atmos. Environ. 185, 243–252. https://doi.org/10.1016/j.atmosenv.2018.04.053.
Mousavi, A., Sowlat, M.H., Lovett, C., Rauber, M., Szidat, S., Boffi, R., Borgini, A., De Marco, C., Ruprecht, A.A., Sioutas, C., 2019. Source apportionment of black carbon (BC) from fossil fuel and biomass burning in metropolitan Milan, Italy. Atmos. Environ. 203, 252–261. https://doi.org/10.1016/j.atmosenv.2019.02.009.
Rai, P., Furger, M., El Haddad, I., Kumar, V., Wang, L., Singh, A., Dixit, K., Bhattu, D., Petit, J.-E., Ganguly, D., Rastogi, N., Baltensperger, U., Tripathi, S.N., Slowik, J.G., Prévôt, A.S.H., 2020. Real-time measurement and source apportionment of elements in Delhi's atmosphere. Sci. Total Environ. 742, 140332. https://doi.org/10.1016/j.scitotenv.2020.140332.
Ramachandran, S., Rajesh, T.A., 2007. Black carbon aerosol mass concentrations over Ahmedabad, an urban location in western India: comparison with urban sites in Asia, Europe, Canada, and the United States. J. Geophys. Res. 112, D06211. https://doi.org/10.1029/2006JD007488.
Ravi Kiran, V., Venkat Ratnam, M., Krishna Murthy, B.V., Kant, Y., Prasad, P., Roja Raman, M., Rao, S.V.B., Lakshmi Kumar, T.V., Maitra, A., 2019. An empirical method for source apportionment of black carbon aerosol: results from Aethalometer observations at five different locations in India. Environ. Pollut. 254, 112932. https://doi.org/10.1016/j.envpol.2019.07.100.
Reddington, C.L., McMeeking, G., Mann, G.W., Coe, H., Frontoso, M.G., Liu, D., Flynn, M., Spracklen, D.V., Carslaw, K.S., 2013. The mass and number size distributions of black carbon aerosol over Europe. Atmos. Chem. Phys. 13, 4917–4939. https://doi.org/10.5194/acp-13-4917-2013.
Russell, P.B., Bergstrom, R.W., Shinozuka, Y., Clarke, A.D., DeCarlo, P.F., Jimenez, J.L., Livingston, J.M., Redemann, J., Dubovik, O., Strawa, A., 2010. Absorption Angstrom Exponent in AERONET and related data as an indicator of aerosol composition. Atmos. Chem. Phys. 10, 1155–1169. https://doi.org/10.5194/acp-10-1155-2010.
Sandradewi, J., Prévôt, A.S.H., Szidat, S., Perron, N., Alfarra, M.R., Lanz, V.A., Weingartner, E., Baltensperger, U., 2008. Using aerosol light absorption measurements for the quantitative determination of wood burning and traffic emission contributions to particulate matter. Environ. Sci. Technol. 42, 3316–3323. https://doi.org/10.1021/es702253m.
Saraswat, Arvind, Apte, Joshua S., Kandlikar, Milind, Brauer, Michael, B Henderson, Sarah, Marshall, Julian D., 2013. Spatiotemporal land use regression models of fine, ultrafine, and black carbon particulate matter in New Delhi, India. Environ. Sci. Technol. 47, 12903–12911. https://doi.org/10.1021/es401489h.
Schnaiter, M., 2005. Absorption amplification of black carbon internally mixed with secondary organic aerosol. J. Geophys. Res. 110, D19204. https://doi.org/10.1029/2005JD006046.
Schnaiter, M., Horvath, H., Möhler, O., Naumann, K.-H., Saathoff, H., Schöck, O.W., 2003. UV-VIS-NIR spectral optical properties of soot and soot-containing aerosols. J. Aerosol Sci. 34, 1421–1444. https://doi.org/10.1016/S0021-8502(03)00361-6.
Sharma, M.C., Pandey, V.K., Kumar, R., Latief, S.U., Chakrawarthy, E., Acharya, P., 2018. Seasonal characteristics of black carbon aerosol mass concentrations and influence of meteorology, New Delhi (India). Urban Climate 24, 968–981. https://doi.org/10.1016/j.uclim.2017.12.002.
Singh, R.P., Chauhan, A., 2020. Impact of lockdown on air quality in India during COVID-19 pandemic. Air Qual Atmos Health 13, 921–928. https://doi.org/10.1007/s11869-020-00863-1.
Stocker, T. (Ed.), 2014. Climate Change 2013: the Physical Science Basis: Working Group I Contribution to the Fifth Assessment Report of the Intergovernmental Panel on Climate Change. Cambridge University Press, New York.
Tiwari, Suresh, Kumar Srivastava, Atul, Singh Bisht, Deewan, Parmita, Pragya, Srivastava, Manoj K., D Attri, S, 2013. Diurnal and seasonal variations of black carbon and $PM_{2.5}$ over New Delhi, India: Influence of meteorology. Atmos. Res. 125-126, 50–62. https://doi.org/10.1016/j.atmosres.2013.01.011.
Tiwari, S., Pipal, A.S., Srivastava, A.K., Bisht, D.S., Pandithurai, G., 2015. Determination of wood burning and fossil fuel contribution of black carbon at Delhi, India using aerosol light absorption technique. Environ. Sci. Pollut. Res. 22, 2846–2855. https://doi.org/10.1007/s11356-014-3531-2.
Tobler, A., Bhattu, D., Canonaco, F., Lalchandani, V., Shukla, A., Thamban, N.M., Mishra, S., Srivastava, A.K., Bisht, D.S., Tiwari, S., Singh, S., Močnik, G., Baltensperger, U., Tripathi, S.N., Slowik, J.G., Prévôt, A.S.H., 2020. Chemical characterization of PM2.5 and source apportionment of organic aerosol in New Delhi, India. Sci. Total Environ. https://doi.org/10.1016/j.scitotenv.2020.140924, 140924.
Tyagi, C., Gupta, N.C., Soni, V.K., Sarma, K., 2020. Seasonal variation of black carbon emissions in urban Delhi, India. Environ. Claims J. 32, 101–111. https://doi.org/10.1080/10406026.2019.1699723.
Vaishya, A., Singh, P., Rastogi, S., Babu, S.S., 2017. Aerosol black carbon quantification in the central Indo-Gangetic Plain: seasonal heterogeneity and source apportionment. Atmos. Res. 185, 13–21. https://doi.org/10.1016/j.atmosres.2016.10.001.
Weingartner, E., Saathoff, H., Schnaiter, M., Streit, N., Bitnar, B., Baltensperger, U., 2003. Absorption of light by soot particles: determination of the absorption coefficient by means of aethalometers. J. Aerosol Sci. 34, 1445–1463. https://doi.org/10.1016/S0021-8502(03)00359-8.
Zhang, Y., Gao, T., Kang, S., Sprenger, M., Tao, S., Du, W., Yang, J., Wang, F., Meng, W., 2020. Effects of black carbon and mineral dust on glacial melting on the Muz Taw glacier, Central Asia. Sci. Total Environ. 740, 140056. https://doi.org/10.1016/j.scitotenv.2020.140056.